A COMPARATIVE STUDY OF Cu-RELATED PASMONIC EFFECTS IN ELECTROCHEMICALLY NANOSTRUCTURED $CuInSe_2$ AND $CuGaSe_2$ CRYSTALS

V. V. Ursaki

Institute of Applied Physics, Academy of Sciences of Moldova, Academiei str. 5, Chisinau, MD-2028 Republic of Moldova

(Received June 26, 2013)

Abstract

We study the differences in electrochemical nanostructuring of $CuInSe_2$ and $CuGaSe_2$ crystals. To make the crystals suitable for electrochemical nanostructuring, they are subjected to thermal treatment either in vacuum or in Zn vapors. It is shown that thermal treatment of $CuInSe_2$ crystals in vacuum at 600–700^{o}C is an appropriate procedure for the consequent electrochemical treatment, while treatment in Zn vapors at temperatures higher than 700^{o}C is necessary to make $CuGaSe_2$ crystals suitable for electrochemical nanostructuring. The possibility of luminescence enhancement via thin Cu film deposition onto nanostructured $CuInSe_2$ and $CuGaSe_2$ surfaces is explored.

1. Introduction

Over the last decades, it has been demonstrated that material properties can be engineered by nanostructuring. An accessible and cost-effective approach for nanostructuring, i.e., for tailoring the architecture of macroscopic objects on the nanometer scale is offered by electrochemistry [1, 2]. The approach based on "drilling" pores in semiconductors via anodic etching has been well explored in elementary semiconductors Si [3–5] and Ge [5–7] as well as in binary III–V [2, 5, 8] and II–VI [9–12] semiconductor compounds with a zincblende structure. It was shown that two types of pores can be introduced in III–V semiconductor compounds [2], namely, crystallographically oriented or 'crysto' pores, and current-line oriented or 'curro' pores. Crysto pores grow along the <111>B directions of the zincblende structure and they are usually generated at low anodic current densities due to direct dissolution of the material. The curro pores are generated at relatively high anodic current densities, their growth being mediated by oxide formation and its dissolution at the pore tip. Curro pores are oriented along current lines and usually have a circular shape independent on the crystallographic orientation of the substrate. The property of long-range interaction of curro pores, under certain conditions, leads to the self-arrangement of pores in a two-dimensional hexagonal closed packed lattice [2, 8]. The approach of electrochemical nanostructuring of semiconductors proves to be a strategy for a variety of applications. For instance, semiconductor nanotemplates possessing a periodic spatial distribution of pores may exhibit properties inherent in photonic crystals, with the photonic band-gap depending upon the transverse dimensions of pores and architecture of the skeleton [2]. Porosity can transform indirect band gap materials into direct band gap ones, thus leading to a sharp increase in the intensity of luminescence [13]. Due to giant fluctuations of the electric field of electromagnetic radiation, nanoporous structures exhibit an enhanced nonlinear optical behavior, in particular, strongly enhanced second harmonic generation and THz emission [14, 15].

Moreover, being able to easily accommodate themselves to compression and strain, nanoporous templates play the role of flexible substrates in nanoheteroepitaxy, enabling one to grow high quality dislocation-free epilayers [16]. Because of the nanoscale nature of light absorption and photocurrent generation in solar energy conversion, the advent of methods for controlling inorganic materials on the nanometer scale opens new opportunities for the development of future generations of solar cells [17]. Solar cell technologies, using I-III-VI_2 direct band-gap chalcopyrite semiconductors as the absorber layer, have attracted great interest [18]. $CuInSe_2$-based solar cells are currently demonstrating the leading performance amongst thin-film technologies: 20% conversion efficiency [19] and excellent stability. $CuInSe_2$ is a semiconductor with a direct band gap near 1.05 eV and an absorption coefficient exceeding 10^5 cm^{-1} [20]. In spite of the high value, the achieved conversion efficiency of 20% is still far from the theoretical limit for a one-junction solar cell [21]. This is an indicative of the importance of further technological improvements. As mentioned above, one way of boosting the performance of solar cells consists in microstructuring and nanostructuring of the materials. The idea is to trap more light so that it bounces around inside the cell instead of reflecting back out, since reflection means the loss of the light, which is absorbed to solar cell and generates electric power. Another way of boosting the performance of solar cells is making use of plasmonic effects by deposition of metallic nanostructures. However, the application of electrochemical nanostructuring to ternary materials is a much more complicated task as compared to elementary or binary compounds, since the decomposition of the ternary material is very probable, and electrochemical treatment should be performed at low applied voltage [22, 23].

The goal of this paper is to perform a comparison of the effects of electrochemical treatment upon $CuInSe_2$ and $CuGaSe_2$ crystals and to study the plasmonic effects in nanostructured layers of these materials covered with thin metallic films.

2. Sample preparation and experimental results

$CuInSe_2$ and $CuGaSe_2$ single crystals were grown by chemical vapor transport (CVT) in a closed system using iodine as a transport agent. The polycrystalline material, which was preliminary synthesized in an iodine atmosphere from a stoichiometric mixture of the elemental constituents, was used as the raw charge in the CVT. The iodine concentration was approximately 5 mg cm^{-3}. The system was cooled down slowly at a rate of 10°C/h to avoid straining of the crystals after crystal growth.

Electrochemical treatment for nanostructuring was performed in an electrochemical cell as described elsewhere [15]. A four Pt electrode configuration was used: a reference electrode in the electrolyte, a reference electrode on the sample, a counter electrode, and a working electrode. The area of the sample exposed to the electrolyte solution was 0.1 cm^2. The anodic etching was carried out in a 5% HCl:H_2O electrolyte in the potentiostatic regime at room temperature. The resulting morphology of the etched samples was studied using a TESCAN scanning electron microscope (SEM). The photoluminescence (PL) was excited by a LD Pumped all-solid state MLL-III-532 laser and analyzed through a double spectrometer. The resolution was better than 0.5 meV. The samples were mounted on the cold station of a LTS-22-C-330 cryogenic system.

3. Results and discussion

The as-grown $CuInSe_2$ and $CuGaSe_2$ crystals are n-type with resistivity in the order of 10^5-10^6 Ω·cm and $>10^7$ Ω·cm, respectively. In is known that low-resistivity crystals are required

for nanostructuring by electrochemical treatment. For decreasing the resistivity of the as-grown $CuInSe_2$ and $CuGaSe_2$ crystals, several types of thermal treatment were applied. $CuInSe_2$ crystals with a resistivity of 0.2 Ω·cm were produced by annealing the crystals in vacuum. A similar treatment of $CuGaSe_2$ crystals reduced their resistivity as little as to 40 Ω·cm. For a further decrease in resistivity, the samples were subjected to annealing in Zn vapors. The samples were subjected to annealing during 30 h. The parameters of samples as a function of technological conditions are presented in the table 1.

Table 1. Electrical parameters of $CuInSe_2$ and of $CuGaSe_2$ crystals subjected to different thermal treatment.

$CuInSe_2$	As grown, #1	Annealed in vacuum at 500°C, #2	Annealed in vacuum at 600°C, #3	Annealed in vacuum at 700°C, #4	Annealed in Zn vapors at 600°C, #5	Annealed in Zn vapors at 700°C, #6
ρ (Ω · cm)	$10^5 \div 10^6$	12	0.6	0.2	0.06	0.03
n (cm^{-3})	-	$2\cdot10^{15}$	$5\cdot10^{16}$	$2.1\cdot10^{17}$	$1.1\cdot10^{18}$	$7\cdot10^{18}$
μ ($cm^2/V\cdot s$)	-	250	210	140	90	30
$CuGaSe_2$	As grown, #1	Annealed in vacuum at 500°C, #2	Annealed in vacuum at 600°C, #3	Annealed in vacuum at 700°C, #4	Annealed in Zn vapors at 600°C, #5	Annealed in Zn vapors at 700°C, #6
ρ (Ω · cm)	$> 10^7$	$10^6 \div 10^7$	$10^5 \div 10^6$	40	4	0.15
n (cm^{-3})	-	-	-	$1.1\cdot10^{15}$	$1.4\cdot10^{16}$	$6\cdot10^{17}$
μ ($cm^2/V\cdot s$)	-	-	-	140	110	70

The PL spectrum of the as grown $CuInSe_2$ (sample #1) is presented by curve *1* in Fig. 1a. The spectrum consists of several near-band-edge lines and several deeper PL band at 0.99 eV, 0.97 eV, and 0.96 eV. Among the near-band-edge lines, two most intensive lines at 1.036 eV and 1.028 eV assigned previously as M2 and M5 lines [20] are attributed to the recombination of bound excitons [24, 25], while the band at higher photon energies (1.042 eV) is due to the recombination of free excitons [20]. The bands at 0.99 eV and 0.97 eV have been previously attributed to donor-acceptor transitions involving a shallow donor and different acceptors [26], such as [Cu_{In}–Cu_i] complex and V_{Cu} center [27–29].

Annealing of $CuInSe_2$ crystals in vacuum at 700°C leads to the quenching of the exciton lines and the emergence of a new broad and asymmetric PL band in the near-band-edge region (at 1.058 eV). This PL band is attributed to the band-to-band transitions, since the shift of the maximum and its broadening correlates with the shift of the equilibrium Fermi level [22]. A similar behavior was observed for the near-band-edge PL band in $CuInS_2$ crystals subjected to a similar thermal treatment [23] and in ZnSe single crystals annealed in a Zn melt containing an Al impurity [30]. Note that the near-band-edge PL band is shifted to lower photon energies in

samples annealed in Zn vapors as compared to samples annealed in vacuum [22]. This behavior is explained in terms of the theory of heavily doped semiconductors [31, 32]. According to this theory, the asymmetric shape of PL bands is caused by potential fluctuations in the material due to the high concentrations of charged defects.

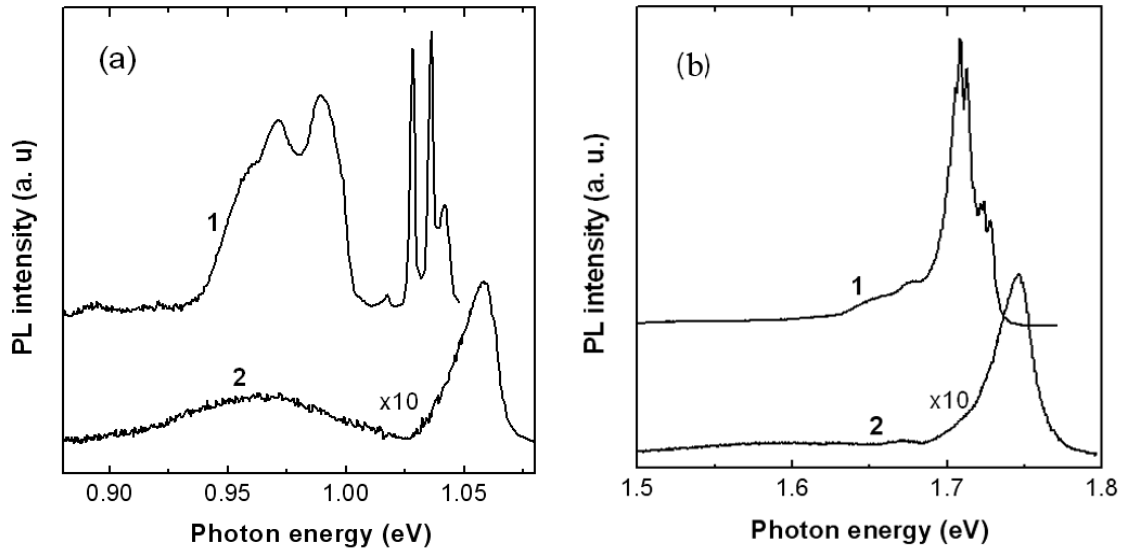

Fig. 1. (a) PL spectra of $CuInSe_2$ crystals with numbers #1 (curve *1*) and #4 (curve *2*); (b) PL spectra of $CuGaSe_2$ crystals with numbers #1 (curve *1*) and #6 (curve *2*). The spectra were measured at $T = 10$ K.

The PL spectrum of the as grown $CuGaSe_2$ (sample #1) is presented by curve *1* in Fig. 1b. This spectrum is dominated by a series of lines due to bound excitons at 1.709 eV, 1.712 eV, 1.721 eV, 1.723 eV, and a peak at 1.727 eV which can be attributed to the recombination of free excitons [33–35]. Two weaker and broader bands are also observed at 1.677 eV and 1.655 eV, which can be associated with donor-acceptor band transitions [35, 36].

In contrast to $CuInSe_2$, annealing of $CuGaSe_2$ crystals in vacuum at 700°C or in Zn vapors at 600°C leads only to a decrease in the luminescence intensity and broadening of the lines related to the recombination of bound excitons and to the disappearance of the band associated with the recombination of free excitons. Similar changes occur in the spectrum of $CuInSe_2$ crystals after annealing in vacuum at 500°C. At the same time, the spectrum of $CuGaSe_2$ crystals annealed in Zn vapors at 700°C (curve *2* in Fig 1b) resembles the spectrum of $CuInSe_2$ crystals annealed in vacuum at 700°C (curve *2* in Fig 1a). That means that the dominating PL band in these samples is caused by potential fluctuations in the material due to the high doping.

The conductivity of samples directly influences the processes of electrochemical etching. The morphology of $CuInSe_2$ samples #3, #4, and #5 from the table after electrochemical treatment under an applied voltage of 0.7 V in an aqueous HCl electrolyte is shown in Fig. 2.

It is evident from Fig. 2 that the formed porous layers have different diameters of pores: around 200 nm for sample #5, 300-400 nm for sample #4, and around 1 μm for sample #3. Therefore, the diameter of pores sharply decreases with increasing conductivity of the material. One can see also from Fig. 2 that some pore merge in sample #4, while in sample #3 several pores merge into a larger unit.

In $CuInSe_2$ sample #6 with the lowest resistivity, a uniform porous structure is formed with a mean dimension of pores around 100 nm as shown in Fig. 3a. At the same time, a non-uniform porosity with pores propagating in different directions is formed in $CuGaSe_2$ sample #6

as shown in Fig. 3b.

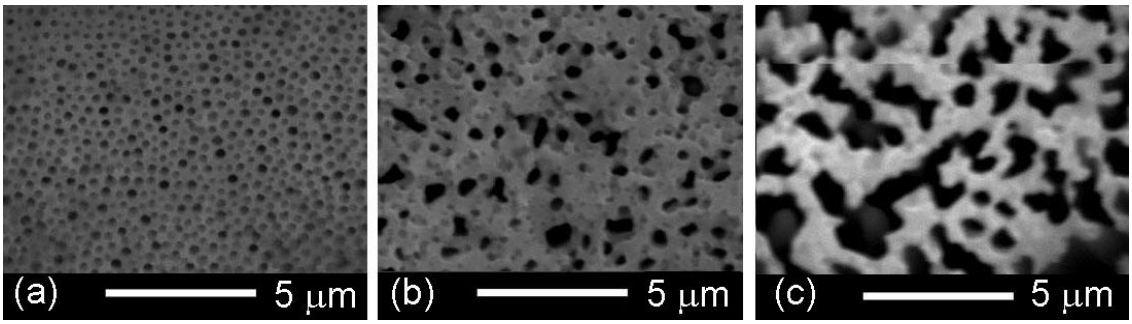

Fig. 2. SEM images of the surfaces of $CuInSe_2$ crystals (a) #5, (b) #4, and (c) #3 in the table subjected to electrochemical treatment at 0.7 V in an aqueous HCl electrolyte.

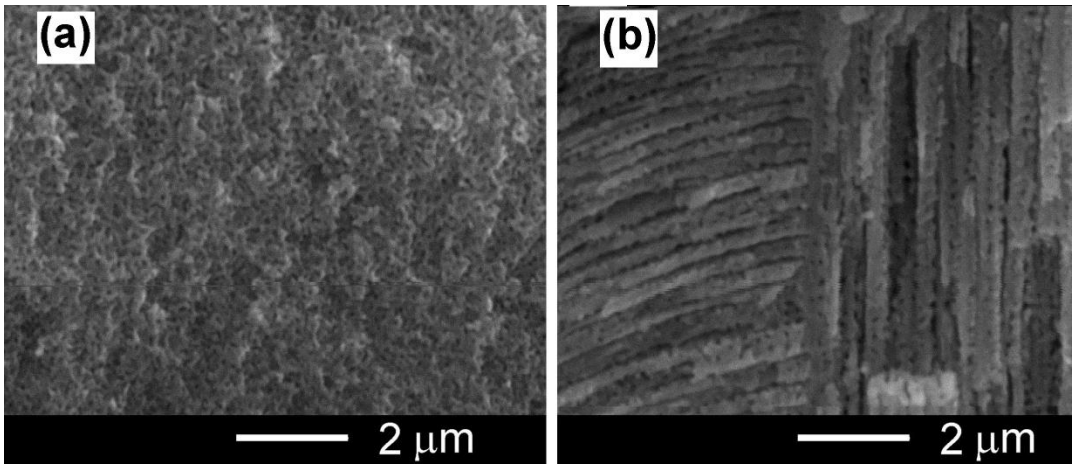

Fig. 3. SEM images in cross section of (a) $CuInSe_2$ (a) and (b) $CuGaSe_2$ crystals with numbers #6 in the table subjected to electrochemical treatment in an aqueous HCl electrolyte.

Thin Cu coatings were deposited onto nanostructured $CuInSe_2$ and $CuGaSe_2$ surfaces by means of a Cressington magnetron sputtering coater in order to study the plasmonic effects in metallized nanostructured ternary chalcogenides. Figure 4 illustrates the effect of deposition of thin Cu films onto $CuGaSe_2$ sample #1 and sample #6.

One can see that deposition of thin Cu films slightly increases the near bandgap luminescence intensity of the as-grown $CuGaSe_2$ sample. The enhancement in PL by Cu films is much more pronounced in $CuGaSe_2$ sample #6, the PL intensity being increased by a factor of 3 after deposition of a Cu film with a thickness of 10 nm. It is suggested that this enhancement is due to surface plasmons. The greater enhancement in sample #6 as compared to as-grown sample #1 is attributed to two causes. Sample #6 is nanostructured, and it is known that nanostructuring enhances plasmonic effects. On the other hand, the energetic position of the PL maximum is shifted to higher photon energies in sample #6 as compared to sample #1; therefore, it is closer to the resonance energy of the surface plasmons in $Cu/CuGaSe_2$.

As concerns the impact of Cu film deposition onto the as grown or nanostructured surfaces of $CuInSe_2$ crystals, no enhancement in PL was observed. On the contrary, deposition of films thicker than 10 nm leads to a decrease in the luminescence intensity due to the absorption of

radiation in the Cu film. The difference in the effect of Cu film deposition on the surfaces of nanostructured $CuInSe_2$ and $CuGaSe_2$ crystals is explained in terms of the difference between the surface plasmon resonance energy in Cu films and the quantum energy of PL bands. The position of PL bands in $CuInSe_2$ is far from the surface plasmon resonance energy at the $Cu/CuInSe_2$ interface.

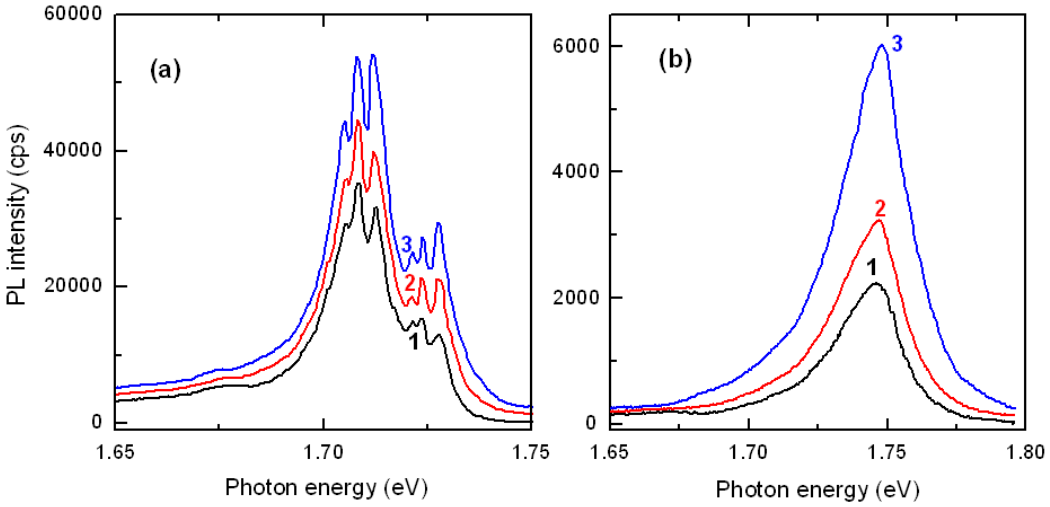

Fig. 4. Low temperature (10 K) PL spectra of $CuGaSe_2$ sample #1 (a) and sample #6 (b): uncovered (curve *1*) and covered with Cu films with a thickness of 5 nm (curve *2*) and 10 nm (curve *3*).

4. Conclusions

The results of this study demonstrate possibilities of producing nanostructured layers in $CuInSe_2$ and $CuGaSe_2$ crystals by means of electrochemical treatment. Thermal treatment under different conditions is needed for both types of materials to control their conductivity before the electrochemical treatment. The studies demonstrate that the treatment of $CuInSe_2$ crystals in vacuum at temperatures of 600–700°C provides conditions for increasing the conductivity of the material to a value suitable for electrochemical nanostructuring. In contrast to that, the treatment of $CuGaSe_2$ crystals under similar conditions does not provide a value of conductivity required for electrochemical treatment, annealing in Zn vapors at 700°C being necessary. The PL spectra of materials are in concordance with the changes in conductivity introduced by thermal treatment, and they can be used for the estimation of the material conductivity. Porous layers with uniform porosity and the diameter of pores controlled in a range of 100 nm to 1 μm can be produced in $CuInSe_2$ crystals, while for $CuGaSe_2$ crystals porosity can be introduced only in crystals subjected to thermal treatment in Zn vapors at 700°C, and the formed porosity is inhomogeneous. The deposition of thin Cu films on nanostructured $CuInSe_2$ surfaces has no effect on their photoluminescence spectra, while the near bandgap luminescence in the region of 1.75 eV from nanostructured $CuGaSe_2$ surfaces is enhanced by a factor of 3 as a result of covering with a 10-nm-thick Cu film. These effects are attributed to the excitation of surface plasmons at the $Cu/CuGaSe_2$ interface.

Acknowledgments. This work was supported by the Academy of Sciences of Moldova, project no. 11.817.05.03A.

References

[1] V. Lehmann. Electrochemistry of silicon. Wiley-VCH, Weinheim, 2002.
[2] H. Föll, S. Langa, J. Carstensen, M. Christophersen, and I. M. Tiginyanu, AdvanceMaterials, 15, 183 (2003).
[3] F. Müller, A. Birner, U. Gösele, V. Lehmann, S. Ottow, and H. Föll, J. Porous. Mater., 7, 201 (2000).
[4] A. Birner, R. Wehrspohn, F. Müller, U. Gösele, and K. Busch, Adv. Mater. (Weinheim, Ger.), 13, 377 (2001).
[5] S. Langa, J. Carstensen, M. Christophersen, K. Steen, S. Frey, I. M. Tiginyanu, and H. Föll, J. Electrochem. Soc, 152, 8, C525 (2005).
[6] S. Miyazaki, K. Sakamoto, K. Shiba, and M. Hirose, Thin Solid Films 255, 99 (1995).
[7] S. Langa, J. Carstensen, I. M. Tiginyanu, and H. Föll, Phys. Status Solidi C, No. 9, 3237 (2005).
[8] S. Langa, I. M. Tiginyanu, J. Carstensen, M. Christophrsen, and H. Föll, Appl. Phys. Lett., 82, 278 (2003).
[9] E. Monaico, V. V. Ursaki, A. Urbieta, P. Fernández, J. Piqueras, R. W. Boyd and I. M. Tiginyanu, Semicond. Sci. Technol. 19, L121 (2004).
[10] I. M. Tiginyanu, E. Monaico, V. V. Ursaki, V. E. Tezlevan, and Robert W. Boyd, Appl. Phys. Lett. 86, 063115 (2005).
[11] E. Monaico, V. V. Ursaki, I. M. Tiginyanu, Z. Dashevsky, V. Kasiyan, and R. W. Boyd, J. Appl. Phys. 100, 053517 (2006).
[12] E. Monaico, I. M. Tiginyanu,V. V. Ursaki, A. Sarua, M. Kuball, D. D. Nedeogli, and V. P. Sirkeli. Semicond. Sci. Technol. 22, 1115 (2007).
[13] A. G. Cullis, L. T. Canham, and P. D. J. Calcott, J. Appl. Phys. 82, 909 (1997).
[14] I. M. Tiginyanu, I. V. Kravetsky, S. Langa, G. Marowsky, J. Monecke, and H. Föll, Phys. Status Solidi A 197, 549 (2003).
[15] M. Reid, I.V. Cravetchi, R. Fedosejevs, I.M. Tiginyanu, L. Sirbu, and Robert W. Boyd, Phys. Rev. B 71, 081306 (2005).
[16] D. Zubia, S. H. Zaidi, S. R. Brueck, and S. D. Hersee, Appl. Phys. Lett. 76, 858 (2000).
[17] W. U. Hyunh, J. J. Dittmer, and A. P. Alivisatos, Science, 295, 2425 (2002).
[18] M. A. Green, K. Emery, D. L. King, S. Igari, and W. Warta, Prog. Photovoltaics 10, 355 (2003).
[19] I. Repins, M. A. Contreras, B. Egaas, C. DeHart, J. Scharf, C. L. Perkins, B. To, and R. Noufi: Prog. Photovoltaics 16, 235 (2008).
[20] M. V. Yakushev, F. Luckert, C. Faugeras, A. V. Karotki, A. V. Mudryi, and R. W. Martin Jpn. J. Appl. Phys. **50**, 05FC03 (2011).
[21] H. W. Schock, Solar Energy Mater. Sol. Cells 34, 19 (1994).
[22] V. V. Ursaki, Mold. J. Phys. Sci. 11, 312 (2012).
[23] E. Monaico, V. Ursaki, V. Zalamai, A. Masnik, N. Syrbu, A. Bullacu, Proc. 7th Int. Conf. Microelectron. Computer Sci., Chisinau, 2011, p. 139.
[24] S. Chatraphorn, K. Yoodee, P. Songpongs, C. Chityuttakan, K. Sayavong, S. Wongmanerod, and P. O. Holtz, Jpn. J. Appl. Phys. 37, L269 (1998).

[25] A. V. Mudriy, I. V. Bodnar, I. A. Viktorov, V. F. Gremenok, M. V. Yakushev, R. D. Tomlinson, A. E. Hill, and R. D. Pilkington, Appl. Phys. Lett. 77, 2542 (2000).
[26] S. Siebentritt and U. Rau (Eds.), "Wide-Gap Chalcopyrites", Chapter 7, Springer (2006).
[27] O. Ka, H. Alves, I. Dirnstorfer, T. Christmann, and B.K. Meyer, Thin Solid Films 361–362, 263 (2000).
[28] S.B. Zhang, S-H. Wei, A. Zunger, and H. Katayama-Yoshida, Phys. Rev. B 57, 9642 (1998).
[29] J. Krustok, A. Jagomagi, J. Raudoja, and M. Altosaar, Solar Energy Mater. Solar Cells 79, 401 (2003).
[30] G. N. Ivanova, D. D. Nedeoglo, N. D. Nedeoglo, V. P. Sirkeli, I. M. Tiginyanu, and V. V. Ursaki. J. Appl. Phys. 101, 063543 (2007).
[31] A. P. Levanyuk and V. V. Osipov, Sov. Phys. Usp. 133, 427 (1981).
[32] B. I. Shklovskij and A. L. Efros, Electronic Properties of Doped Semiconductors, Springer, Berlin, 1984.
[33] A. Bauknecht, S. Siebentritt, J. Albert, Y. Tomm, and M. Ch. Lux-Steiner, Jpn. J. Appl. Phys. 39 (Suppl.), 322 (2000).
[34] A. Yamada, Y. Makita, S. Niki, A. Obara, P. Fons, H. Hajime, M. Kawai, S. Chichibu, and H. Nakanishi, J. Appl. Phys. 79 4318 (1996).
[35] Meeder, A. Jager-Waldau, V. Tezlevan, E. Arushanov, T. Schedel-Niedrig, and M. Ch. Lux-Steiner, J. Phys.: Condens. Matter 15, 6219 (2003).
[36] A. Meeder, D. Fuertes Marron, V. Tezlevan, E. Arushanov, A. Rumberg, T. Schedel-Niedrig, and M. Ch. Lux-Steiner MCh, Thin Solid Films 431/432, 214 (2003).